MRAS Sensorless Vector Control of an Induction Motor Using New Sliding Mode and Fuzzy Logic Adaptation Mechanisms

S. M. Gadoue, *Member, IEEE*, D. Giaouris, *Member, IEEE*, and J.W. Finch, *Senior Member, IEEE*

***Abstract*-- Two novel adaptation schemes are proposed to replace the classical PI controller used in model reference adaptive speed estimation schemes which are based on rotor flux. The first proposed adaptation scheme is based on sliding mode theory. A new speed estimation adaptation law is derived using Lyapunov theory to ensure estimation stability as well as fast error dynamics. The other adaptation mechanism is based on fuzzy logic strategy. A detailed experimental comparison between the new and conventional schemes is carried out in both open and closed loop sensorless modes of operation when a vector control drive is working at very low speed. Superior performance has been obtained using the new sliding mode and fuzzy logic adaptation mechanisms in both modes of operations.**

***Index Terms*-- Fuzzy control, Induction motors, Model reference adaptive control, Sliding mode control.**

I. Nomenclature

i_{sD}, i_{sQ}	Stator current components in the stator frame
J	Rotor inertia
L_m	Mutual inductance
L_s, L_r	Stator and rotor self inductances
p	Differential operator
R_s, R_r	Stator and rotor resistances
T_r	Rotor time constant
v_{sD}, v_{sQ}	Stator voltage components in the stator frame
ε_ω	Speed tuning signal
σ	Leakage coefficient
ψ_{rd}, ψ_{rq}	Components of the rotor flux linkage vector
ω_r	Angular rotor speed

Manuscript received July 17, 2009.

Shady Gadoue is with the Department of Electrical Engineering, Faculty of Engineering, Alexandria University, 21544, Alexandria, Egypt. Damian Giaouris and John W. Finch are with the School of Electrical, Electronic and Computer Engineering, Newcastle University, Newcastle upon Tyne, NE1 7RU, England, UK. (e-mail: {Shady.Gadoue, Damian.Giaouris, J.W.Finch}@ncl.ac.uk)

II. Introduction

Several strategies have been proposed for rotor speed estimation in sensorless induction motor drives [1]. Among these techniques Model Reference Adaptive Systems (MRAS) schemes are the most common strategies employed due to their relative simplicity and low computational effort [1, 2]. Rotor flux, back EMF and reactive power techniques are popular MRAS strategies which have received a lot of attention. The back EMF scheme may have stability problems at low stator frequency and show low noise immunity but avoids pure integration. The reactive power method is characterized by its robustness against stator resistance variation while avoiding pure integration but suffers from instability [2, 3]. Therefore rotor flux MRAS, first proposed by Schauder [4], is the most popular MRAS strategy and a lot of effort has been focused on improving the performance of this scheme. Generally the main problems associated with the low speed operation of model based sensorless drives are related to machine parameter sensitivity, stator voltage and current acquisition, inverter nonlinearity and flux pure integration problems [1, 5]. Since all model based estimation techniques rely on rotor induced voltages which are very small and even vanish at zero stator frequency, these techniques fail at or around zero speed [5].

PI controllers are widely used in industrial control systems applications. They have a simple structure and can offer a satisfactory performance over a wide range of operation. Therefore, the majority of adaptation schemes described in the literature for MRAS speed observers employ a simple fixed gain linear PI controller to generate the estimated rotor speed. However, due to the continuous variation in the machine parameters and the operating conditions in addition to the nonlinearities present in the inverter, fixed gain PI controllers may become unable to provide the required performance. Adaptive control techniques, such as gain scheduling, where the PI gains vary with the operating conditions, are often used to improve the controller performance. Not much attention has been devoted to study other types of adaptation mechanisms used to minimize the speed tuning signal to obtain the estimated speed.

In this paper this point is addressed by presenting two novel nonlinear adaptation mechanisms to replace the classical PI controller used in the conventional rotor flux based-MRAS speed observer. A novel nonlinear adaptation scheme based on Sliding Mode (SM) theory is proposed to improve the speed estimation performance. The new speed estimation adaptation law, which ensures estimation stability and fast error dynamics, is derived based on Lyapunov theory. Furthermore, a Fuzzy Logic Controller (FLC) is proposed as another nonlinear optimizer to minimize the speed tuning signal used for the rotor speed estimation. The performance of the new and conventional schemes is compared based on detailed experimental tests in both open loop and sensorless modes of operation. Focus is given to operation at low speed which represents a critical region of operation for a MRAS observer.

III. Rotor Flux MRAS Speed Observer

The classical rotor flux MRAS speed observer shown in Fig.1 consists mainly of a reference model, an adaptive model and an adaptation scheme which generates the estimated speed. The reference model, usually expressed by the voltage model, represents the stator equation. It generates the reference value of the rotor flux components in the stationary reference frame from the monitored stator voltage and current components. The reference rotor flux components obtained from the reference model are given by [4, 6]:

$$p\psi_{rd} = \frac{L_r}{L_m}\left\{ v_{sD} - R_s i_{sD} - \sigma L_s p i_{sD} \right\} \tag{1}$$

$$p\psi_{rq} = \frac{L_r}{L_m}\left\{ v_{sQ} - R_s i_{sQ} - \sigma L_s p i_{sQ} \right\} \tag{2}$$

The adaptive model, usually represented by the current model, describes the rotor equation where the rotor flux components are expressed in terms of stator current components and the rotor speed. The rotor flux components obtained from the adaptive model are given by [4, 6]:

$$p\hat{\psi}_{rd} = \frac{L_m}{T_r} i_{sD} - \frac{1}{T_r}\hat{\psi}_{rd} - \hat{\omega}_r \hat{\psi}_{rq} \tag{3}$$

$$p\hat{\psi}_{rq} = \frac{L_m}{T_r} i_{sQ} - \frac{1}{T_r}\hat{\psi}_{rq} + \hat{\omega}_r \hat{\psi}_{rd} \tag{4}$$

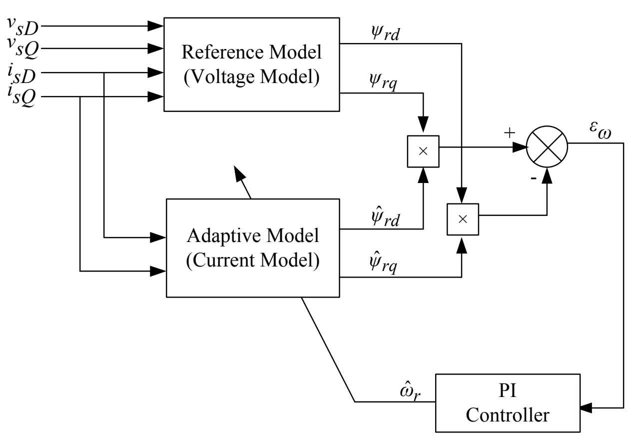

Fig. 1 Conventional MRAS speed observer

Finally the adaptation scheme generates the value of the estimated speed to be used in such a way as to minimize the error between the reference and estimated fluxes. In the classical rotor flux MRAS scheme, this is performed by defining a speed tuning signal, ε_ω, to be minimized by a PI controller which generates the estimated speed which is fed back to the adaptive model. The expressions for the speed tuning signal and the estimated speed can be given as [6]:

$$\varepsilon_\omega = \psi_{rq}\hat{\psi}_{rd} - \psi_{rd}\hat{\psi}_{rq} \tag{5}$$

$$\hat{\omega}_r = \left(k_p + \frac{k_i}{p} \right)\varepsilon_\omega \tag{6}$$

IV. Sliding Mode MRAS Speed Observer

Sliding Mode Control (SMC) is a variable structure control with high frequency discontinuous control action which switches between several functions depending on the system states [7]. It can be one of the most effective and robust control strategies in addition to its capability to cope with bounded disturbance as well as model imprecision which makes it suitable for robust nonlinear control of induction motor drives. Mathematical basics, design procedures and applications of SMC in electric drives have been covered in [7]. The principle of SMC is to define a switching control law to drive the nonlinear state trajectory onto a switching surface and to maintain this trajectory sliding on this surface for all subsequent time[8]. The control law is defined based on Lyapunov theory to guarantee the motion of the state trajectory towards the sliding surface. This is done by choosing a hitting control gain to maintain the derivative of Lyapunov function always negative definite [9].

The classical SM strategy applied for control applications is modified here to fit with the speed estimation problem. Hence a novel SM rotor flux MRAS (MRAS-SM) is developed to replace the conventional constant gain PI controller. A new speed estimation adaptation law for the SM scheme is derived based on Lyapunov theory to ensure stability and fast error dynamics. Defining the speed tuning signal (5) and choosing a sliding surface s as:

$$s = \varepsilon_\omega + \int k\varepsilon_\omega \, dt \quad k > 0 \tag{7}$$

Such that the error dynamics at the sliding surface $s = 0$ will be forced to exponentially decay to zero. When the system reaches the sliding surface, this gives:

$$\dot{s} = \dot{\varepsilon}_\omega + k\varepsilon_\omega = 0 \tag{8}$$

and the error dynamics can be described by:

$$\dot{\varepsilon}_\omega = -k\varepsilon_\omega \tag{9}$$

The SM control law can be found using Lyapunov theory and defining the Lyapunov function candidate [9]:

$$v = \frac{1}{2}s^2 \tag{10}$$

According to Lyapunov theory, if the function $\dot{v}$ is negative definite, this will ensure that the state trajectory will be driven and attracted toward the sliding surface s and once reached, it will remain sliding on it until the origin is reached asymptotically [9]. The time derivative of the Lyapunov function in (10) can be calculated as:

$$\dot{v} = s\,\dot{s} \Leftrightarrow s\left(\dot{\varepsilon}_\omega + k\varepsilon_\omega\right) \tag{11}$$

Differentiating (5) yields:

$$\dot{\varepsilon}_{\omega} = \dot{\psi}_{rq}\hat{\psi}_{rd} + \psi_{rq}\dot{\hat{\psi}}_{rd} - \dot{\psi}_{rd}\hat{\psi}_{rq} - \psi_{rd}\dot{\hat{\psi}}_{rq} \tag{12}$$

Substituting the current model (3-4) into (12) yields:

$$\begin{aligned}\dot{\varepsilon}_{\omega} &= \dot{\psi}_{rq}\hat{\psi}_{rd} - \dot{\psi}_{rd}\hat{\psi}_{rq} + \frac{L_m}{T_r} i_{sD}\psi_{rq} - \frac{1}{T_r}\hat{\psi}_{rd}\psi_{rq} \\ &\quad - \frac{L_m}{T_r} i_{sQ}\psi_{rd} + \frac{1}{T_r}\hat{\psi}_{rq}\psi_{rd} - \hat{\omega}_r\left(\psi_{rq}\hat{\psi}_{rq} + \psi_{rd}\hat{\psi}_{rd}\right)\end{aligned} \tag{13}$$

By letting:

$$\begin{aligned} f_1 &= \dot{\psi}_{rq}\hat{\psi}_{rd} - \dot{\psi}_{rd}\hat{\psi}_{rq} + \frac{L_m}{T_r} i_{sD}\psi_{rq} - \frac{1}{T_r}\hat{\psi}_{rd}\psi_{rq} \\ &\quad - \frac{L_m}{T_r} i_{sQ}\psi_{rd} + \frac{1}{T_r}\hat{\psi}_{rq}\psi_{rd}\end{aligned} \tag{14}$$

$$f_2 = \psi_{rq}\hat{\psi}_{rq} + \psi_{rd}\hat{\psi}_{rd} \tag{15}$$

Equation (13) can be written as:

$$\dot{\varepsilon}_{\omega} = f_1 - \hat{\omega}_r f_2 \tag{16}$$

and (8) can be written as:

$$\dot{s} = f_1 + k\varepsilon_{\omega} - \hat{\omega}_r f_2 \tag{17}$$

Substituting (17) into (11) yields:

$$\dot{v} = s\left(f_1 + k\varepsilon_{\omega} - \hat{\omega}_r f_2\right) \tag{18}$$

This derivative is negative definite if:

$$\left(f_1 + k\varepsilon_{\omega} - \hat{\omega}_r f_2\right) \begin{array}{ll} < 0 & for\ s > 0 \\ = 0 & for\ s = 0 \\ > 0 & for\ s < 0 \end{array} \tag{19}$$

This can be ensured if:

$$\hat{\omega}_r = \frac{f_1 + k\varepsilon_{\omega}}{f_2} + M\ sign(s) \quad M > 0 \tag{20}$$

where the sign function is defined as:

$$sign(s) = \begin{Bmatrix} -1 & for\ s < 0 \\ +1 & for\ s > 0 \end{Bmatrix} \tag{21}$$

Equation (20) represents the switching law of the SM controller and could be written in general form as:

$$\hat{\omega}_r = u_{eq} + u_s \tag{22}$$

where u_{eq} is the equivalent control which defines the control action that keeps the state trajectory on the sliding surface, u_s is the switching control which depends on the sign of the switching surface and M is the hitting control gain which makes (11) negative definite [9]. No design criterion is assigned to choose the value of M; however, its value should be selected high enough to make the manifold $s = 0$ in (7) attractive [9, 10]. Therefore the control law defined in (20) will guarantee the existence of the switching surface s in (7) and when the error function ε_{ω} reaches the sliding surface, the system dynamics will be governed by (9) which is always stable [11]. The expressions for the equivalent and the switching control functions can be written as:

$$u_{eq} = \frac{f_1 + k\varepsilon_{\omega}}{f_2} \tag{23}$$

$$u_s = M\ sign(s) \quad M > 0 \tag{24}$$

The presence of the function f_2 in the denominator of the equivalent control u_{eq} may cause problems in the estimation performance of the proposed scheme if its value approaches zero. This problem can be avoided by allowing magnetizing of the machine before starting up and by adding a positive small value to f_2. The use of the sign function in the SM control (20) causes high frequency chattering due to the discontinuous control action which represents a severe problem when the system state is close to the sliding surface [9]. The block diagram of the novel MRAS observer employing SM adaptation mechanism (MRAS-SM) is shown in Fig. 2.

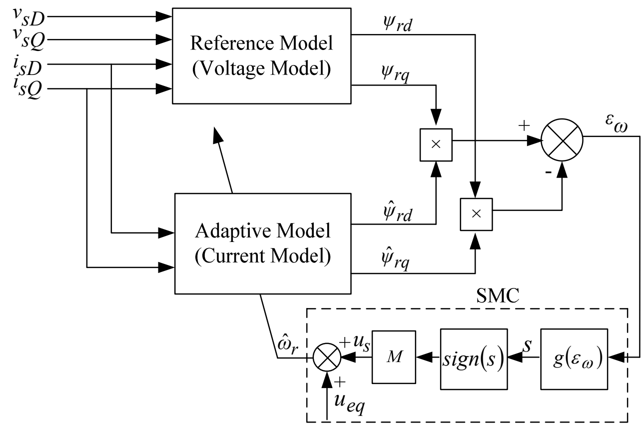

Fig. 2 MRAS-SM speed observer

V. Fuzzy Logic MRAS Speed Observer

Various applications of FL have shown a fast growth in the last few years. FLC has become popular in the field of industrial control applications for solving control, estimation and optimization problems [12]. In this section FL is proposed to replace the PI controller used for error minimization in the conventional MRAS speed observer.

FL technique has been applied to solve optimization problems for induction motor drives [13-17]. It has been proposed to replace PI controllers in different error minimization applications [18, 19]. For the MRAS speed observer, the mechanism of the estimation of the rotor speed can be regarded as an optimization problem where the PI controller is generating a quantity, the estimated speed, in such a way as to minimize a specified error, which is the speed tuning signal in (5), in a feedback loop. Therefore, FLC can replace the conventional PI controller to solve the optimization problem.

The proposed FLC is a Mamdani-type rule base where the inputs are the speed tuning signal ε_{ω} in (5) and its change $\Delta\varepsilon_{\omega}$ which can be defined as:

$$\Delta\varepsilon_{\omega}(k) = \varepsilon_{\omega}(k) - \varepsilon_{\omega}(k-1) \tag{25}$$

These two inputs are multiplied by two scaling factors k_e and k_d respectively. The output of the controller is multiplied by a third scaling factor k_u to generate the actual value of the rate of change of the estimated speed. Finally, a discrete integration is performed to get the value of the estimated speed. Hence a PI-Type FLC is created where the expression for the estimated speed can be written as:

$$\hat{\omega}_r(k) = \hat{\omega}_r(k-1) + \Delta\hat{\omega}_r(k) \tag{26}$$

The choice of the values of the scaling factors greatly affects the performance of the FLC. A trial and error technique is usually used to tune these gains to ensure optimal performance of the controller [16]. Each variable of the FLC has seven membership functions. The following fuzzy sets are used: NB= NEGATIVE BIG, NM= NEGATIVE MEDUIM, NS= NEGATIVE SMALL, ZE= ZERO, PS= POSITIVE SMALL, PM= POSITIVE MEDUIM, PB= POSITIVE BIG. The universe of discourse of the inputs and outputs of the FLC are chosen between -0.1 and 0.1 with triangular membership functions as shown in Fig. 3. Table 1 shows the fuzzy rule base with 49 rules [16]. FLC is modeled using the Matlab Fuzzy Logic Toolbox graphical user interface (GUI). The overall MRAS speed observer with FL speed estimation mechanism (MRAS-FL) is shown in Fig. 4.

TABLE I

Linguistic rule base for PI-Type fuzzy logic controller

$\Delta\varepsilon_\omega$ \ ε_ω	**NB**	**NM**	**NS**	**ZE**	**PS**	**PM**	**PB**
NB	NB	NM	NM	NS	NS	NS	ZE
NM	NM	NM	NS	NS	NS	ZE	PS
NS	NM	NM	NS	NS	ZE	PS	PM
ZE	NB	NM	NS	ZE	PS	PM	PM
PS	NS	NS	ZE	PS	PS	PM	PM
PM	NS	ZE	PS	PS	PS	PM	PM
PB	ZE	PS	PS	PM	PM	PB	PB

VI. THE EXPERIMENTAL SYSTEM

The experimental platform, shown in Fig. 5, consists of a 7.5 kW, 415 V, delta connected three phase induction machine loaded by a 9 kW, 240 V, 37.5 A separately excited DC load machine to allow separate control of torque and speed of the DC machine. A 15 kW four quadrant DC drive from the Control Techniques “Mentor” range is used to control the DC machine to provide different levels of loading on the induction machine up to full load. The induction machine parameters are given in the Appendix.

The AC drive power electronics consists of a 50A 3 Phase Diode Bridge and 1200V, 50A half bridge IGBT power modules. To control the induction motor a dSPACE DS1103 control board is used which consists of a Power PC 604e processor running at 400 MHz, and a Slave Texas Instruments TMS320F240 DSP.

Hall effect current sensors were used to measure the motor line currents. The actual motor speed is measured by a 5000 pulses/revolution incremental optical encoder. The rotor speed measurement is to allow standard *encodered* vector control operation and is employed as a reference for sensorless operation. The inverter switching frequency is 15 kHz, with a dead time period of 1.5 μs, and the vector control is executed with the same sampling frequency. The observer and the speed control loop have a sampling frequency of 5 kHz and the speed measurement is executed with a sampling frequency of 250 Hz.

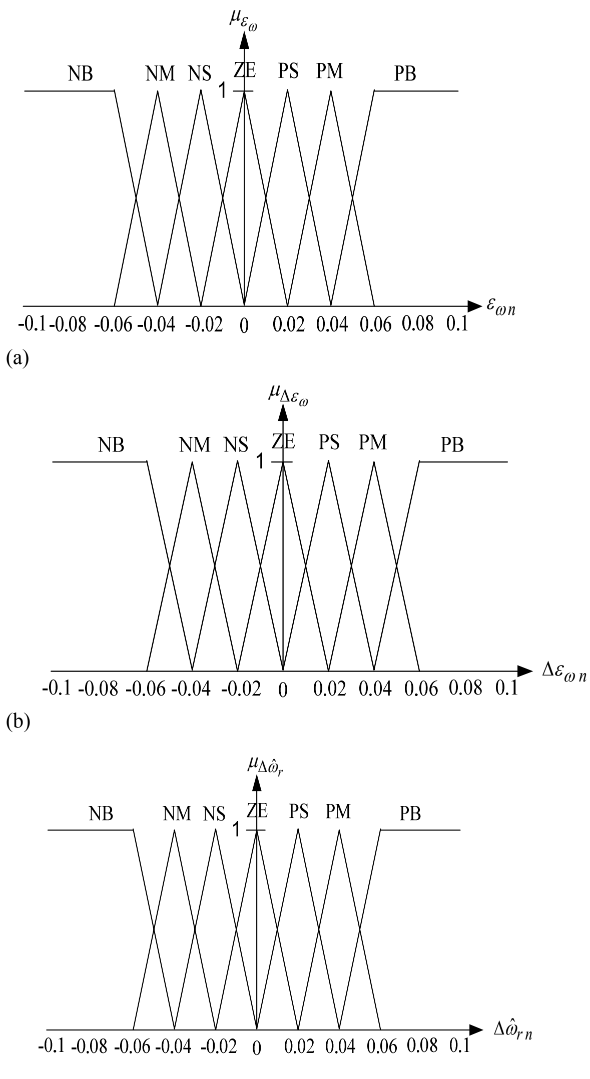

Fig. 3 Fuzzy controller input and output membership functions (a) error (b) error change (c) change in the estimated speed

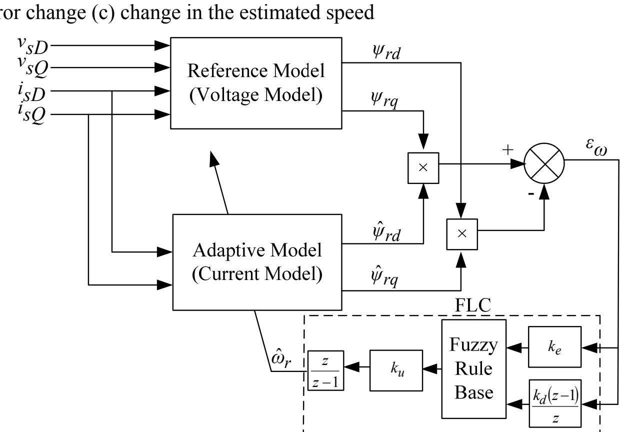

Fig. 4 MRAS-FL speed observer

During practical implementation of the MRAS scheme it was found necessary to cascade a low cut-off frequency high pass filter at the outputs of the voltage model to remove integrator drift and any initial condition problems. The cut-off frequency should be selected as low as possible since the purpose is just to remove the DC component and therefore a value of 1 Hz is chosen.

A simple dead time compensator similar to [20, 21] is implemented and reference voltages which are available in the control unit are used to avoid the need to measure the real stator voltages and will be used for the voltage model flux observer in (1) and (2).

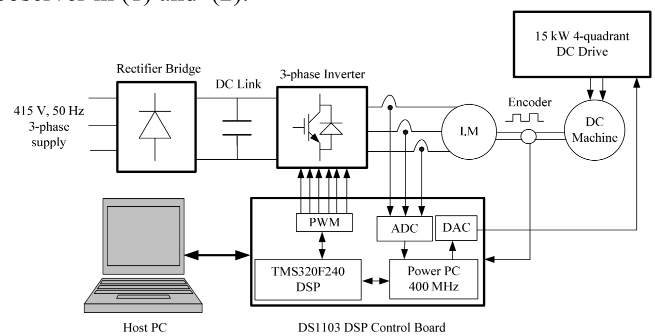

Fig. 5 The Experimental Platform

To use the FLC in real time with the dSPACE card and Simulink, a two dimensional look-up table is generated from the FL toolbox in Matlab with a step size of 0.0005 for the inputs. The FLC implementation using a look-up table is shown in Fig. 6 where the saturation limits for the input saturation blocks are set to 0.1 and -0.1.

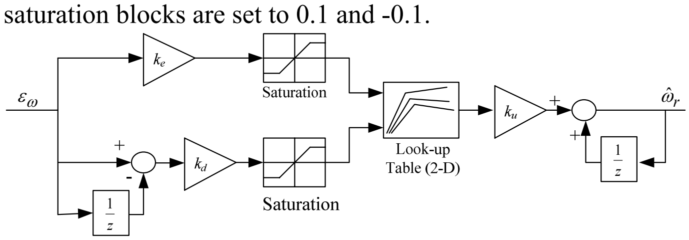

Fig. 6 FLC implementation using look-up tables

VII. Experimental Results

Extensive experimental tests were carried out to compare the three adaptation schemes; PI, FL and SM using an indirect vector control IM drive. The tests were performed in both open loop and sensorless modes of operation.

A. Open loop performance

The three adaptation mechanisms were tested in open loop when the drive is operated as an *encodered* vector control, i.e. the encoder speed is used for speed control and rotor flux angle estimation. The drive was subjected to different reference speed changes at various load torque levels. The PI controller gains can be selected as high as possible but are limited by the noise [6]. PI gains of K_p = 10; K_i = 100, obtained by trial and error, were shown to provide an optimal performance for the conventional MRAS observer. Although fixed gains are used in this work, it would be possible to obtain better performance if variable gains via gain scheduling technique are employed. To allow a fair comparison FLC gains were tuned in such a way as to obtain similar steady state performance as with the PI controller and are found to be: k_e = 0.01; k_d = 1; k_u = 5.

A LPF is a natural solution to reducing the chattering in the estimated speed obtained from the SM scheme. Using high order sliding mode should also reduce this chattering. The LPF also removes the spikes that may appear in the estimated speed due to the differentiation of fluxes in (14). The choice of the cut-off frequency for this LPF affects the observer performance. Using small values reduces the speed ripples but introduces more delay in the estimated speed. A cut-off frequency of 30 rad/s was found to be a good compromise between speed ripples and dynamic response. The parameters of the SMC are: k = 1000; M = 0.1 and are obtained by trial and error.

At low speed a steady state error in the estimated speed is observed for the MRAS observer using the three adaptation schemes. This is mainly due to the stator resistance mismatch between the motor and the observer. Moreover, since dead time effects cannot be completely removed even by complicated compensation schemes [5], the reference voltages used for the voltage model did not match the actual stator voltages across the machine terminals which represents another source for the steady state error in the estimated speed.

Figs. 7-13 show the performance of the three schemes for 25% load torque disturbance rejection at 60 rpm, speed change from 30 rpm to 100 rpm at 25% load and for speed change from 50 rpm to 100 rpm at rated load.

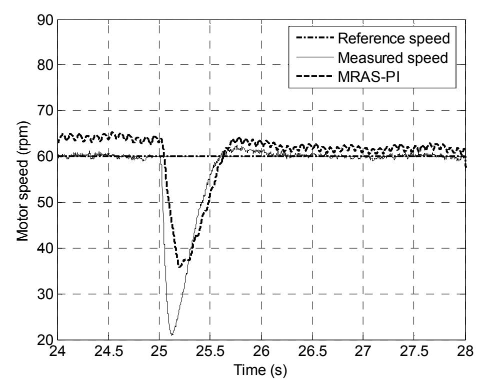

(a)

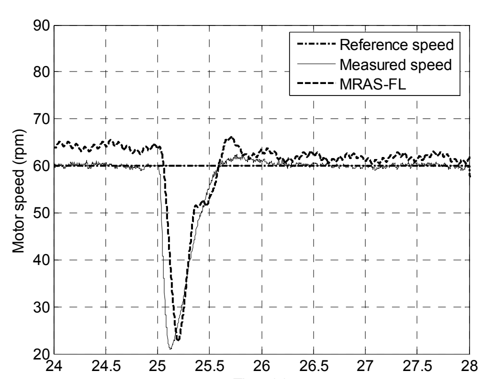

(b)

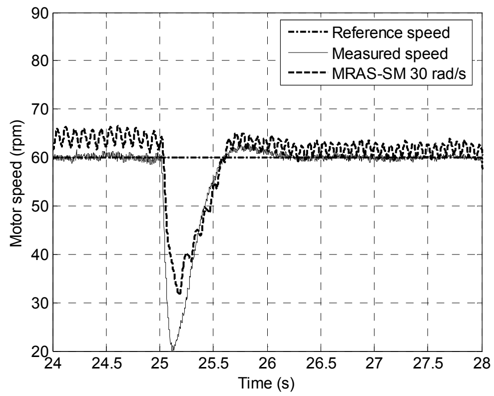

(c)

Fig. 7 Speed estimation performance for 25% load disturbance rejection at 60 rpm (a) MRAS-PI (b) MRAS-FL (c) MRAS-SM

FL and SM schemes show better transient response compared to the PI scheme, which is due to an optimal speed tuning signal during transients as shown in Figs. 8, 9 and 12. The switching surface of the SM scheme (7) corresponding to the unfiltered speed is shown in Figs. 10, 13. These figures show that the manifold $s=0$ is attractive causing fast error dynamics.

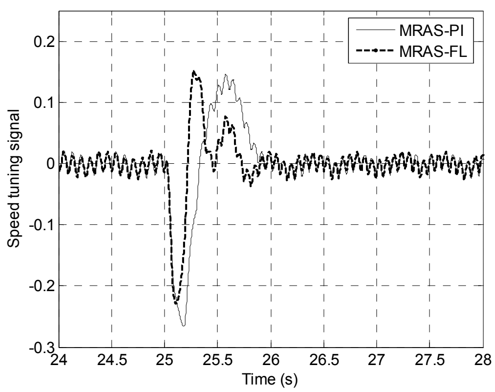

(a)

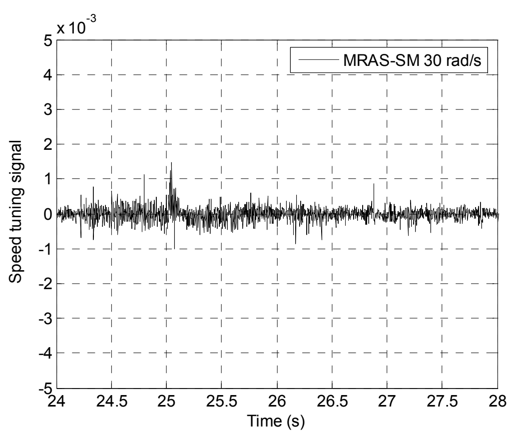

(b)

Fig. 8 Speed tuning signal for 25% load disturbance rejection (a) PI and FL (b) SM

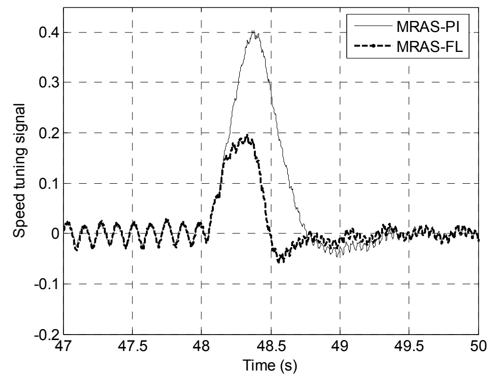

Fig. 9 Speed tuning signal for speed change at 25% load

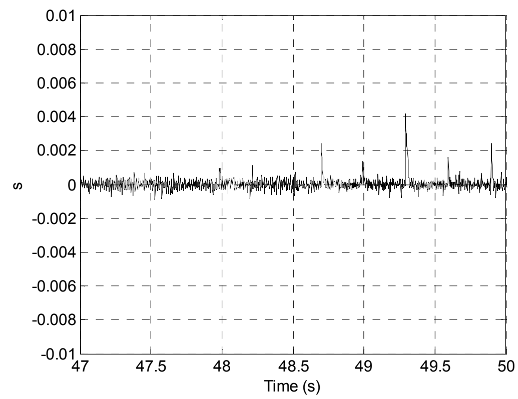

Fig. 10 Switching surface of SM scheme for speed change at 25% load

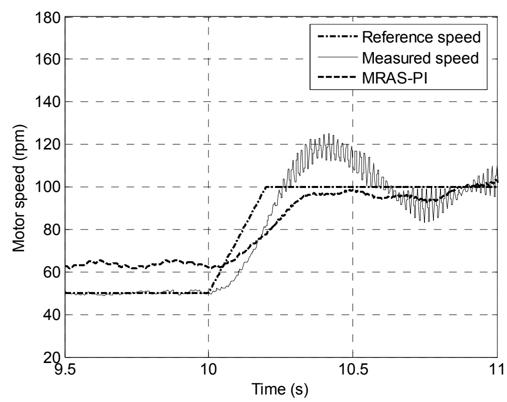

(a)

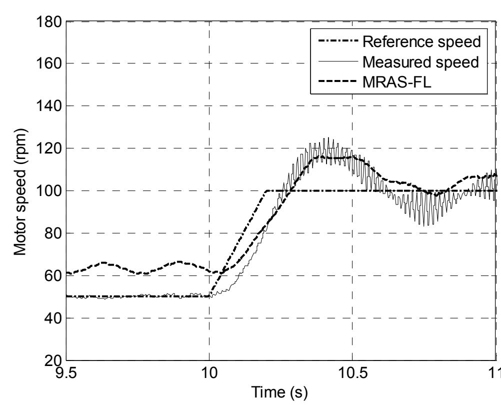

(b)

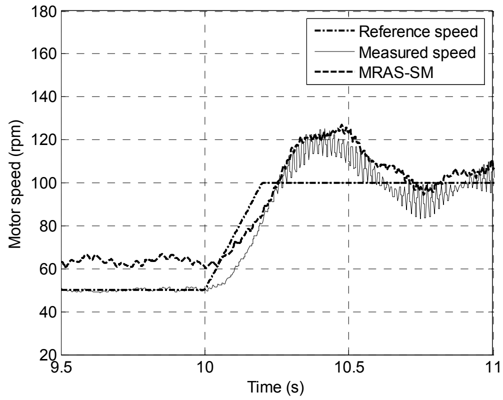

(c)

Fig. 11 Speed estimation performance at rated load (a) MRAS-PI (b) MRAS-FL (c) MRAS-SM

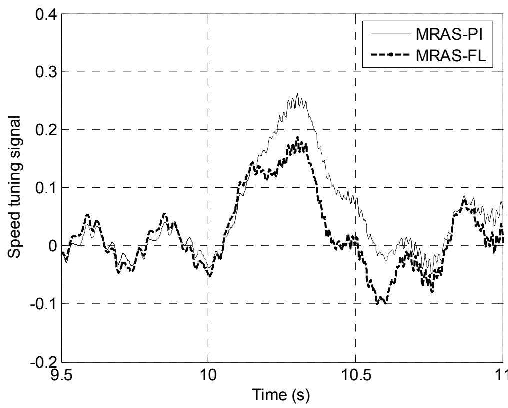

Fig.12 Speed tuning signal for rated load test

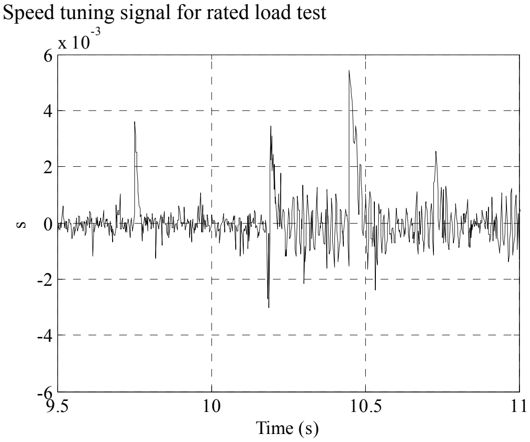

Fig. 13 Switching surface of SM scheme at rated load

B. Sensorless performance

In these tests, the vector control drive is working in the closed loop sensorless mode where the estimated speed is used for both speed control and rotor flux orientation. The three schemes are compared when the drive is running at different operating conditions at very low speed.

Sensorless performance of all schemes is shown in Figs. 14-18 where the drive is subjected to reference speed change from 40 rpm to 100 rpm at no load and 25% load torque application at 100 rpm. Compared to the PI scheme, FL and SM still show a faster response during transients. Moreover, the FL scheme shows faster response compared to the SM scheme due to the need for LPF for the SM scheme. An optimal speed tuning signal was obtained for the FL scheme compared to the PI scheme as shown in Figs. 15, 17. The switching surface of the SM scheme for the 25% load disturbance rejection test is shown in Fig. 18.

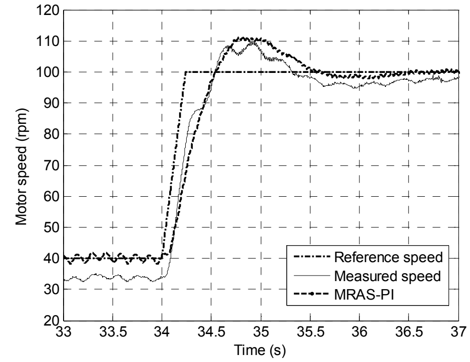

(a)

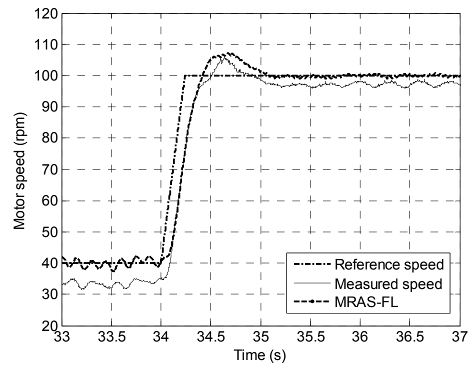

(b)

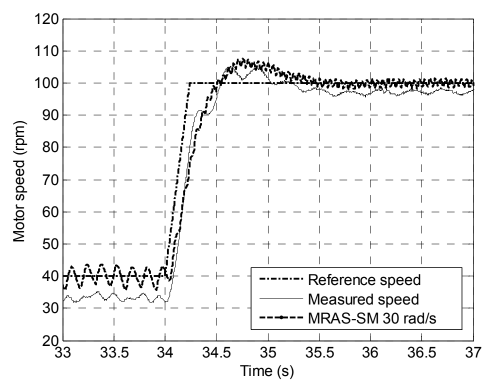

(c)

Fig. 14 Sensorless performance at no load (a) MRAS-PI (b) MRAS-FL (c) MRAS-SM

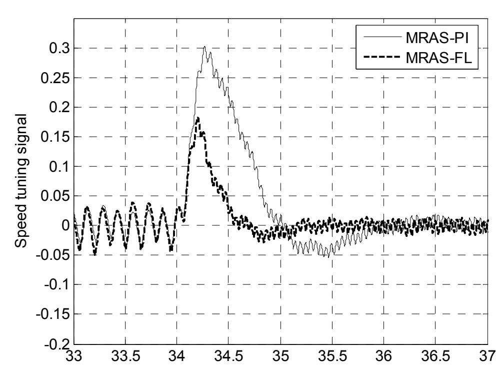

Fig. 15 Speed tuning signal during sensorless no-load operation

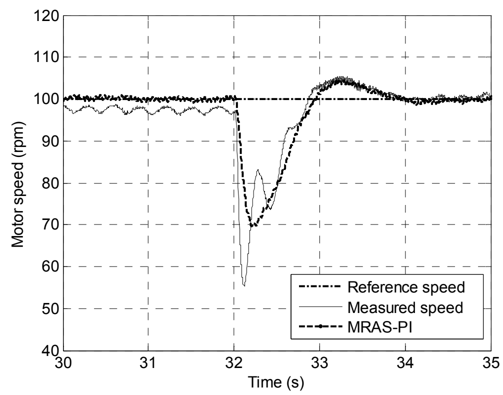

(a)

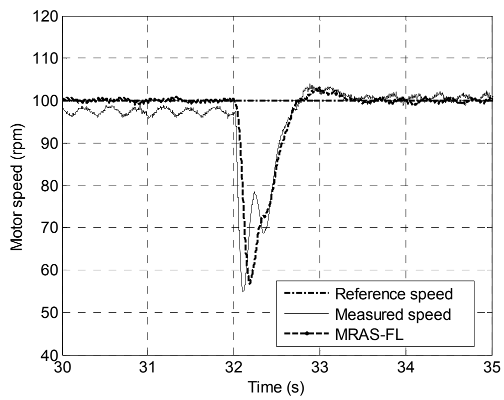

(b)

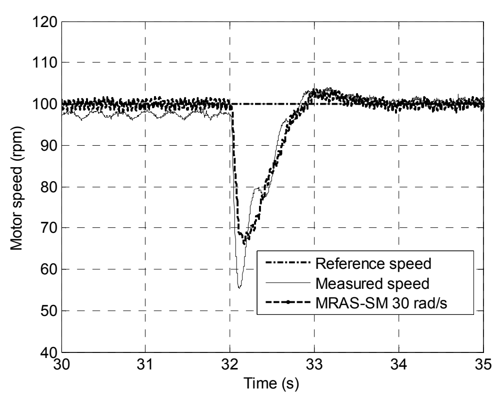

(c)

Fig. 16 Sensorless performance for 25% load disturbance rejection (a) MRAS-PI (b) MRAS-FL (c) MRAS-SM

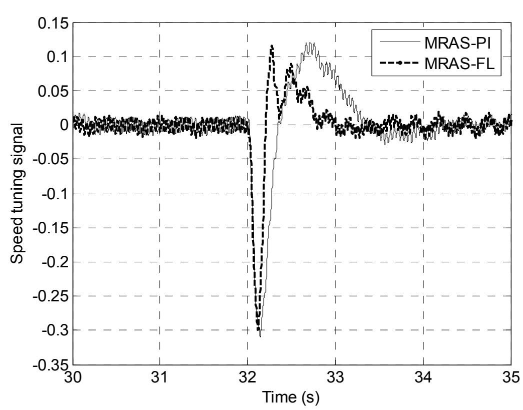

(a)

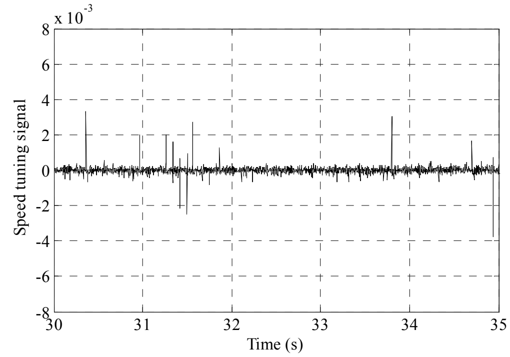

(b)

Fig. 17 Speed tuning signal during sensorless load torque rejection (a) PI and FL (b) SM

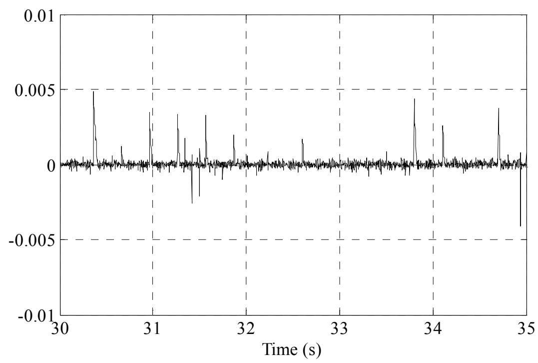

Fig. 18 Switching surface for SM scheme during sensorless load torque rejection

VIII. Conclusion

In this paper two novel nonlinear adaptation mechanisms are proposed to replace the fixed gain PI controller which is conventionally used for rotor flux MRAS observer. One of these schemes is based on SM theory where a novel speed estimation adaptation law is derived based on Lyapunov theory to ensure estimation stability with fast error dynamics. The second scheme is based on a FL strategy working in a nonlinear optimization mode. Parameter tuning of the PI and FL schemes has been performed in such a way as to obtain similar steady state performance. A detailed experimental comparison between the three schemes has been carried out using an indirect vector control induction motor drive. Application of the new schemes shows better transient performance as well as better load torque disturbance rejection in both open loop and closed loop sensorless modes of operation. More specifically, due to the need of low pass filtering of the estimated speed obtained from the SM approach, the FL strategy shows a faster response than the SM scheme. However, the application of the new adaptation schemes does not considerably improve the steady state performance.

IX. Appendix

Motor Parameters

7.5 kW, 3-phase, 415V, delta connected, 50 Hz, 4 pole, Star equivalent parameters: $R_s = 0.7767\ \Omega$, $R_r = 0.703\ \Omega$, $L_s = 0.10773$ H, $L_r = 0.10773$ H, $L_m = 0.10322$ H, $J = 0.22$ kgm^2

References

[1] J. W. Finch and D. Giaouris, "Controlled AC Electrical Drives," *IEEE Transactions on Industrial Electronics*, vol. 55, no. 1, pp. 1-11, February 2008.

[2] M. Rashed and A. F. Stronach, "A stable back-EMF MRAS-based sensorless low speed induction motor drive insensitive to stator resistance variation," *IEE Proceedings Electric Power Applications*, vol. 151, no. 6, pp. 685-693, November 2004.

[3] Y. A. Kwon and D. W. Jin, "A novel MRAS based speed sensorless control of induction motor," in *Proc. the 25th Annual Conference of the IEEE Industrial Electronics Society*, 1999, pp. 933-938.

[4] C. Schauder, "Adaptive speed identification for vector control of induction motors without rotational transducers," *IEEE Transactions on Industry Applications*, vol. 28, no. 5, pp. 1054-1061, September/October 1992.

[5] J. Holtz and J. Quan, "Drift and parameter compensated flux estimator for persistent zero stator frequency operation of sensorless controlled induction motors," *IEEE Transactions on Industry Applications*, vol. 39, no. 4, pp. 1052-1060, July/August 2003.

[6] P. Vas, *Sensorless Vector and Direct torque control.* New York: Oxford University Press, 1998.

[7] V. Utkin, "Sliding mode control design principles and applications to electric drives," *IEEE Transactions on Industrial Electronics*, vol. 40, no. 1, pp. 23-36, February 1993.

[8] W. S. Levine, *The control handbook.* Boca Raton, FL: CRC Press, 1996.

[9] J. Lo and Y. Kuo, "Decoupled fuzzy sliding-mode control," *IEEE Transactions on Fuzzy systems*, vol. 6, no. 3, pp. 426-435, August 1998.

[10] M. Comanescu and L. Xu, "Sliding mode MRAS speed estimators for sensorless vector control of induction machine," *IEEE Transactions on Industrial Electronics*, vol. 53, no. 1, pp. 146-153, February 2006.

[11] K. Shyu and H. Shieh, "A new switching surface sliding-mode speed control for induction motor drive systems," *IEEE Transactions on Power Electronics*, vol. 11, no. 4, pp. 660-667, July 1996.

[12] P. Vas, *Artificial-Intelligence-Based Electrical Machines and Drives-Application of Fuzzy, Neural, Fuzzy-Neural and Genetic Algorithm Based Techniques.* New York: Oxford University Press, 1999.

[13] F. Zidani, M. Nait-Said, M. Benbouzid, D. Diallo, and R. Abdessemed, "A Fuzzy Rotor Resistance Updating Scheme for an IFOC Induction Motor Drive," *IEEE Power Engineering Review*, vol. 21, no. 11, pp. 47-50, November 2001.

[14] E. Bim, "Fuzzy optimization for rotor constant identification of an indirect FOC induction motor drive," *IEEE Transactions on Industrial Electronics*, vol. 48, no. 6, pp. 1293-1295, December 2001.

[15] M. Ta-Cao and H. Le-Huy, "Rotor resistance estimation using fuzzy logic for high performance induction motor drives," in *Proc. The 24th Annual Conference of the IEEE Industrial Electronics Society*, 1998, pp. 303 - 308.

[16] Y. Miloud and A. Draou, "Fuzzy logic based rotor resistance estimator of an indirect vector controlled induction motor drive," in *Proc. IEEE 28th Annual Conference of the Industrial Electronics Society*, 2002, pp. 961 - 966.

[17] B. Karanayil, M. Rahman, and C. Grantham, "Stator and rotor resistance observers for induction motor drive using fuzzy logic and artificial neural networks," *IEEE Transactions on Energy Conversion*, vol. 20, no. 4, pp. 771-780, December 2005.

[18] S. Mir, M. E. Elbuluk, and D. S. Zinger, "PI and fuzzy estimators for tuning the stator resistance in direct torque control of induction machines," *IEEE Transactions on Power Electronics*, vol. 13, no. 2, pp. 279-287, March 1998.

[19] B. Karanayil, M. F. Rahman, and C. Grantham, "PI and fuzzy estimators for on-line tracking of rotor resistance of indirect vector controlled induction motor drive," in *Proc. IEEE International Electric Machines and Drives Conference*, 2001, pp. 820-825.

[20] S. H. Kim, T. S. Park, J. Y. Yoo, G. T. Park, and N. J. Kim, "Dead time compensation in a vector-controlled induction machine," in *Proc. Power Electronics Specialists Conference*, 1998, pp. 1011-1016.

[21] L. Ben-Brahim, "On the compensation of Dead Time and Zero-Current crossing for a PWM-Inverter-controlled AC servo drive," *IEEE Transactions on Industrial Electronics*, vol. 51, no. 5, pp. 1113-1117, October 2004.

Biography

Shady M Gadoue (M'06) was born in Cairo, Egypt, in 1978. He received the B.Sc. (with honors), and the M.Sc. degrees in Electrical Engineering from the Faculty of Engineering, Alexandria University, Egypt in 2000 and 2003, respectively, and the Ph.D. degree in the area of Sensorless control of Induction Motor drives from Newcastle University, UK in 2009. He is with the Department of Electrical Engineering, Alexandria University, where he worked as a Demonstrator in 2000 and an Assistant Lecturer in 2003 and is currently a Lecturer on electrical machines and drives. His main research interests are in the area of estimation and control in electric drives and power electronics. His current research activities relate to sensorless control of induction motor drives using artificial intelligence techniques.

Damian Giaouris (M'01) was born in Munich, Germany, in 1976. He received the Diploma in 620 automation engineering from the Automation Department, Technological Educational Institute of Thessaloniki, Thessaloniki, Greece, in 2000, and the M.Sc. degree in automation and control with distinction and the Ph.D. degree in the area of control and stability of induction machine drives from Newcastle University, Newcastle upon Tyne, U.K., in 2001 and 2004, respectively. He is currently a Lecturer on control systems with the School of Electrical, Electronic and Computer Engineering, Newcastle University. His research interests are advanced nonlinear control, estimation, and digital signal processing methods applied to electric drives and electromagnetic devices, and nonlinear phenomena in power electronic converters.

John W. Finch (M'90-SM'92) was born in Durham, U.K. He received the B.Sc.(Eng.) degree (with first class honors) in electrical engineering from University College London (UCL), London, U.K., and the Ph.D. degree from the University of Leeds, Leeds, U.K. He was a Consultant to many firms and was an Associate Director with the Resource Centre for Innovation and Design, helping companies with developments. He is currently Emeritus Professor of electrical control engineering with the School of Electrical, Electronic and Computer Engineering, Newcastle University, Newcastle upon Tyne, U.K. He has authored or coauthored 150 publications on applied control and simulation of electrical machines and drives. Prof. Finch was a winner of the Goldsmid Medal and Prize (UCL Faculty prize), the Carter Prize (Leeds University postgraduate prize), and the IET's Heaviside, Kelvin, and Hopkinson Premiums. He is an IET Fellow and is also a Chartered Engineer in the U.K.